Investigation of the feasibility of SPR as a method for detection of Troponin-I by antibody binding for whole blood analysis

Semester: Nano 9 & 10
Morten G. Poulsen

P9 & P10-Period: The 1th of August 2009 to the 30th of June 2010

AALBORG UNIVERSITET

Department of Physics and Nanotechnology
Skjernvej 4A
9220 Aalborg Øst
Denmark
Phone Tlf. +45 9940 9215
Fax +45 9815 6502
http://www.physics.aau.dk

Title: Investigation of the feasibility of SPR as a method for detection of Troponin-I by antibody binding for whole blood analysis.

Project period:
P9 and P10,
Start: 1^{nd} of August 2009
End: 30^{th} of June 2010

Participants:
Morten Gravgaard Poulsen

Supervisors:
Leonid Gurevich

Print run: 6

Number of pages: 32

Number of appendices: 2

Date finished: 30^{th} of June 2010

Abstract:

In this Project an introduction and further theoretical description of Surface Plasmon Resonance (SPR) is presented. A matlab program has been written for a theoretical model of a multilayer SPR surface, and this is utilised for investigation of the succes of antibody immobilisation. A method for manufacturing SPR surfaces from a polished glass wafer is presented, and a procedure for immobilising antibodies on this surface is presented. This procedure is utilised to create a biosensor against cardiac Troponin I (cTnI), and this sensor is tested. A commercial available SPR chip (Xantec SPR sensor chip CMD500l) is also tested and found to provide more reproducible data. When testet on cTnI diluted in bovine serum albumin, the sensor gives poor results. It is concluded that more experiments with different pH values and different coatings are needed.

Preface

This report is the product of the 9th and 10th semester project at the Department of Physics and Nanotechnology at Aalborg University. The report is written in the project period from the 1^{nd} of August 2009 to the 30^{th} of June 2010.

References are given using the following system: If the reference is for a single sentence, it is placed before the full stop. If the reference refers to the whole section or paragraph, the reference is placed after the full stop of that section or paragraph. The full bibliography can be found at the end of the report.

I would like to thank Thomas Søndergaard for assistance with the Matlab program.

Morten Gravgaard Poulsen

Contents

Introduction 1

Surface Plsamon resonance (SPR) is an optical method for detection of changes in the refractive index near the interface between a metal and a dielectric. In a typical SPR setup, the metal is gold, and the dielectric is a buffer or an organic solution.

The first observation of SPR dates back to 1902, where dark lines were observed in a diffraction spectrum by Wood. The next reported observation was in 1958, when a drop in the reflection profile of a thin metal film was observed by Thurbadar. Since the early 1990s [1], SPR sensors have been commercially available, and as optical techniques have been improved, their sensitivity have improved as well. The detection limit of this kind of sensor is in the range of 20 to 50 $ng\ cm^{-2}$ [2], but are depending on the specific set-up. [3]

Generally there are five set-ups for excitation of surface plasmons; the angle modulation, the wavelength mo-dulation, the intensity modulation, the phase modulation and the polarization modulation [3]. For the angle modulation method, there are three set-ups utilizing either: prisms, gratings or optical wave guides. In the prism setup, a gold layer is placed on a prism which splits up the indecent light beam, thus providing a broad range of angles of illumination on the gold layer. The reflected light is detected by a CCD chip after leaving the prism, resulting in an angle versus intensity output. This set-up is also called the Kretschmann configuration [4].

For the actual detection, there are two general categories: direct or indirect measurement. In the direct measurement, the analyte is brought into vicinity of the gold surface, and the association of analyte onto the surface can be measured. For the indirect measurement, the surface is treated with a coupling agent, e.g. an antibody. There are several ways to bind the coupling agent to the surface, but the most common are by an aktin/biotin interaction, a dextran matrix, an hydrogel, or by binding it to a mercapto acid. If antibodies specific to a metabolite is immobilised on the gold surface, a highly sensitive and specific biosensor is obtained.

Acute Myocardiac Infarction

Acute myocardial infarction (AMI) is a condition that affects more than 1 million people each year in the US alone, and approximately 34% of these are fatal [5]. To be able to administer the correct treatment, fast and reliable diagnostic methods are needed. The metabolites cardiac Troponin I (cTnI) and cardiac Troponin T (cTnT) are at all times present in the blood serum at small concentrations, but when the cardiac cells enter a necrotic stage, these proteins will, among others, be released into the bloodstream. This rise in Troponin concentration occurs within a few hours after an AMI, and the concentration stays elevated for several days. cTnI is a 29 kDa protein, and, as souch, a rather small protein, whereas cTnT is 39.7 kDa [6]. Troponins can, however, be released by other conditions than AMI, and therefore the concentrations of both proteins need to be known in order to give the correct diagnosis.

To determine the concentration of cTnI in a blood sample, standard methods use antibodies specific for cTnI, where a label have been chemically bound

to the antibody. Examples of such labels are horseradish peroxidase or radioactive isotopes [1]. This method is known as Enzyme-linked immunosorbent assay (ELISA), and involves two binding periods, one to bind the metabolite to the primary antibody, and one to bind the secondary antibody to the metabolite.

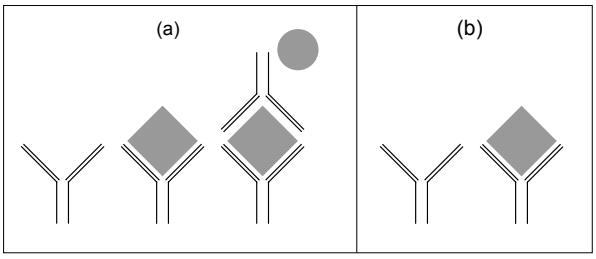

Figure 1.1: (a) A representation of an ELISA assay. First the antigen (square) is bound to the immobilised antigen, then a secondary antibody is introduced, which also binds to the antigen, and carry a reporter molecule (circle). (b) A representation of the set-up used in SPR immuno assay. The immobilised antibody binds the antigen, and the change in mass is measured as a change in SPR response.

Aim or project

By utilising an SPR immuno assay with antibodies specific to cTnI a label free online detector could be obtained, thus removing the need for the secondary binding period. This could drastically improve the diagnosis time.

In this project a sensor will be sought constructed as to provide the means to investigate the feasibility, selectivity and reproducibility of such a sensor.

Theory 2

2.1 Antibodies

Antibodies, or immunoglobulins, are large proteins utilised by the immune system of mammalians for the purpose of identifying and neutralising foreign elements. There are five types of immunoglobulin, each having a specific role in either the production of new antibodies or in the defence against foreign elements. The type of antibody that recognises foreign elements and signal for them to be neutralised is called Immunoglobulin G (IgG). [7]

IgG is build up of two heavy chains (each 50 kD) and two light chains (each 25 kD). Half of the two heavy chains are linked together in two β sheet sandwich motives, and each of the other halves of the heavy chains are linked with a light chain in a similar β sheet sandwich motive. This produces a 'Y' shaped structure, where most of the structure is highly conserved except for 6 loops at each end of the 'arms'. These hyper variable loops are what give the antibodies the unique property to recognise foreign elements. There are three loops on the heavy chain and three loops on the light chain, and each loop contains of between 5 and 17 residues, although the third loop on the heavy chain can contain up to 27 residues. The physical size of an antibody can be estimated from a crystallografic structure determination to a length of 14 nm. and if the structure is 'flattened' the thickness is approximately 7.5 nm [8]. [7, 9]

The production of antibodies was first made viable in 1975 by Kohler and Milstein, as they described a method for isolating antibody producing B-lymphocytes from the Blood of antigen inoculated mammals. This was done by fusing them with myeloma cells, and subsequently purifying them in a limiting growth medium, only allowing for fused cells to reproduce. This produces a polyclonal antibody culture, as a mammalian immune system produces several different antibodies against different epitopes on the same antigen. An ELISA essay is then used to isolate a monoclonal antibody (mAb) producing culture, by dilution to very low cell density . [10]

The uses for antibodies is diverse, and have had a great influence in the development of optical biosensors. In resent development researchers have been

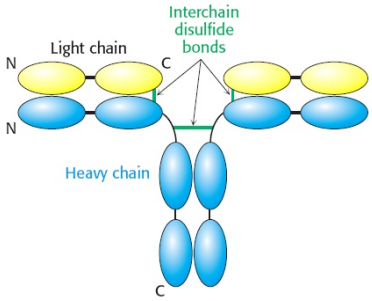

Figure 2.1: A schematic representation of an Immunoglobulin G (IgG). The two heavy chains are shown in blue and the light chains are shown in yellow. The two arms are not locked in a specific position.

exploring the use of antibodies in the detection of biomarkers associated with diseases ranging from cancer [11] to tuberculosis [12]. Other areas of research are also exploring the advantages of the selectivity of antibodies, as they are being explored for use in detection of explosives for use in homeland securiety [13], as well as detection of illegal drugs [14].

2.2 Introducing the Surface plasmon wave

The surface plasmon wave is described as an electromagnetic wave propagating along the interface between a metal (gold) and a dielectricum (buffer or water). To explain how surface plasmons occur, an analysis of the electromagnetic properties of the interface is necessary. In such an analysis a key component is the dispersion relation, which describes the relation between the wave vector k and the angular frequency ω, and this will be derived in the following.

When working with electromagnetic fields (EM-fields) the central concept is the electric wave equation:

$$\nabla^2 \vec{E} - \frac{\epsilon}{c^2} \frac{\partial^2 \vec{E}}{\partial t^2} = 0 \tag{2.1}$$

This is derived from the Maxwell equations under assumption that ϵ is constant on the scale of one wavelength. For the purpose of solving the wave equation, it is assumed that all electromagnetic waves solving this equation have a harmonic time dependence:

$$\vec{E}(\vec{r}, t) = \vec{E}(r) e^{-i\omega t} \tag{2.2}$$

Using this in equation 2.1, the time derivation can be solved, and thus the equation is reduced to:

$$\nabla^2 \vec{E}(\vec{r}) + k_0^2 \epsilon \vec{E} = 0 \tag{2.3}$$

where k_0 is the propagation vector in vacuum $\left(\frac{\omega}{c}\right)$. A simple idealised set-up could be described as two partially infinite mediums (1 and 2) where medium one is a metal characterised by a dielectric constant ϵ_1 and the other medium is a dielectric with dielectric constant ϵ_2. The two mediums are arranged so that the interface between the two is in the x, y plane. This means that dielectric constant only is a function of z. Furthermore, the geometry is arranged so that the $\vec{E}$ field is propagating along the x axis, orthogonal to the y axis, making this a two dimensional problem. This gives us the possibility to write the E field as:

$$\vec{E}(x, y, z) = \vec{E}(z) e^{ik_x x} \tag{2.4}$$

Here k_x is the propagation vector in the x direction. This is used to further simplify the wave equation, by reducing the Laplace operator to the second derivative in the z direction:

$$\frac{\partial^2 \vec{E}(z)}{\partial z^2} + (k_0^2 - \beta^2)\vec{E} = 0 \tag{2.5}$$

As the electric and the magnetic fields are coupled, a similar wave equation exists for the magnetic field, though it is not displayed here.

A deeper differential analysis will show that only transverse magnetic or p-polarised modes give non-zero results, when determining eigenstates for the resonance waves. These eigenstates are governed by the following two equations, which are derived from the curl equations of the maxwell's equations:

$$E_x = -i\frac{1}{\omega\epsilon_0\epsilon}\frac{\partial H_y}{\partial z} \tag{2.6}$$

$$E_z = -\frac{k_x}{\omega\epsilon_0\epsilon}H_y \tag{2.7}$$

and the wave equation for the y component of the H field:

$$\frac{\partial^2 H_y}{\partial z^2} + (k_0^2\epsilon - k_x^2)H_y = 0 \tag{2.8}$$

Solving this equation provides the following formula for $H_y(z)$:

$$H_y(z) = \begin{cases} Ae^{ik_x x}e^{k_{z1}z} & , \quad \text{for } z < 0 \\ Ae^{ik_x x}e^{-k_{z1}z} & , \quad \text{for } z > 0 \end{cases} \tag{2.9}$$

Using this in equation 2.6 and 2.7 gives the equations that describes the E field at the interface:

$$E_x(z) = \begin{cases} -iA\frac{1}{\omega\epsilon_0\epsilon_1}k_{z,1}e^{ik_x x}e^{k_{z,1}z} & , \quad \text{for } z < 0 \\ iA\frac{1}{\omega\epsilon_0\epsilon_2}k_{z,2}e^{ik_x x}e^{-k_{z,2}z} & , \quad \text{for } z > 0 \end{cases} \tag{2.10}$$

$$E_z(z) = \begin{cases} -A\frac{k_x}{\omega\epsilon_0\epsilon_1}e^{ik_x x}e^{k_{z,1}z} & , \quad \text{for } z < 0 \\ -A\frac{k_x}{\omega\epsilon_0\epsilon_2}e^{ik_x x}e^{-k_{z,2}z} & , \quad \text{for } z > 0 \end{cases} \tag{2.11}$$

Border conditions at the interface demands continuity in the magnitude of the H_y field as well as $\epsilon_i E_z$, and thus the values of the constants 'A' have the same value. This continuity also sets a requirement for the relationship between the z components of the wave vector and the relationship between the dielectric constants:

$$\frac{k_{z,2}}{k_{z,1}} = -\frac{\epsilon_2}{\epsilon_1} \tag{2.12}$$

This is one of two relations needed to obtain a dispersion relation for the surface plasmon waves. The other relation is obtained by inputting the equation for H_y (eq. 2.9 into the waveequation (eq. 2.8):

$$k_1^2 = k_x^2 - k_0^2\epsilon_1 \tag{2.13}$$

$$k_2^2 = k_x^2 - k_0^2\epsilon_2 \tag{2.14}$$

Combining these last three equations and the definition of the vacum propagation vector $k_0 = \frac{\omega}{c}$ gives us the dispersion relation:

$$k_x = \frac{\omega}{c}\sqrt{\frac{\epsilon_1\epsilon_2}{\epsilon_1 + \epsilon_2}} \tag{2.15}$$

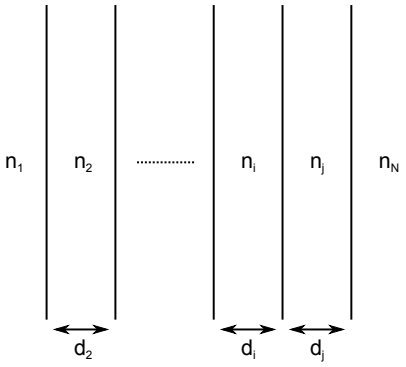

Figure 2.2: The model used in the matrix method for multiple beam interference. The electric field travels from the left to the right through the mediums characterised by their refractive indexes n. Derived from [16]

From this it can be seen that the angular frequency is depending on the dielectric constant, and thus the refractive index, as $\epsilon = n^2$. [15, 4]

This derivation is, however, rather basic, as it is only valid for an interface with only metal and dielectricum. The set-up utilised in a SPR sensor is composed of multiple layers, and thus a more complex method is needed to correctly describe the expected signal.

2.3 SPR in multiple layer interface

In order to obtain a theoretical model of a SPR profile, a matrix method for multiple-beam interference is used. The following derivation is based on the work made by Klein and Furtak [16].

The purpose of this section is to attain an expression that describes the reflection from an SPR interface. To achieve this, three steps are required. Firstly, the refracted and reflected parts of an indecent wave needs to be expressed as a function of the incoming wave. Secondly, the obtained equations should be combined to a matrix set-up, where a single matrix describes the transition over an interface. Thirdly, this should also be done for the transition through a medium, and finally these matrices can be utilised to create a single matrix describing multiple stacked mediums, which can be used to give the reflection from the sum of the interfaces.

The derivation takes basis in the relation between the incoming EM field, the field transmitted through the interface, and the reflected field:

$$E_{rj} = E'_{ri}\tau_{ij} + E_{lj}\rho_{ji} \tag{2.16}$$

The constants τ_{ij} and ρ_{ji} are the transmission and the reflection coefficient of the interface between medium i and j respectively. E_{rj} is the electric field (E field) travelling to the right in the medium j, just on the right side of the interface (see fig. 2.3). E'_{ri} is the E field travelling to the right in the medium i, just to the left of the interface. E_{lj} is then the field travelling to the left in the medium j, on the right of an interface. If the incident EM wave is p-polarized, such that the E field is in the plane of incidence, τ_{ij} and ρ_{ji} is given by:

$$\tau_{ij} = \frac{2(\tilde{n_i}/\tilde{n_j}')}{1+b} \tag{2.17}$$

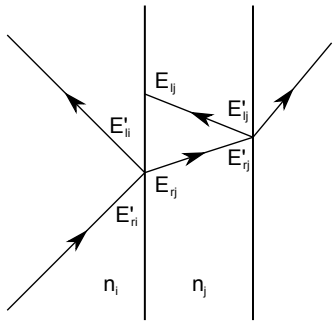

Figure 2.3: A detailed model of the optical situation that is analysed in sec. 2.3. The electric field travels from the left (E'_{ri} to the right through the mediums characterised by their refractive indexes n_i and n_j. Derived from [16]

and

$$\rho_{ji} = \frac{1-b}{1+b} \tag{2.18}$$

where

$$b = \left(\frac{\tilde{n}_i}{\tilde{n}_j}\right)^2 \left(\frac{k_{z,j}}{k_{z,i}}\right) \tag{2.19}$$

and $\tilde{n}_i$ and $\tilde{n}_j$ is the complex refractive index of medium i and j. $k_{z,j}$ is the reciprocal wave number of the E field in medium j. As with E_{rj} (eq. 2.16), the electric field travelling to the left in medium i, can be expressed as:

$$E'_{li} = E_{lj}\tau_{ji} + E'_{ri}\rho ij \tag{2.20}$$

By combining eq. 2.16 and eq. 2.20 E'_{ri} can be eliminated from eq. 2.16:

$$E'_{li} = \left(\frac{\tau_{ji}\tau_{ij} - \rho_{ji}\rho_{ij}}{\tau_{ij}}\right) E_{lj} + E_{rj}\frac{\rho_{ij}}{\tau ij} \tag{2.21}$$

The expression in the brackets can further be reduced by utilising the relations: $\rho_{ij} = -\rho_{ji}$ and $\tau_{ji}\tau_{ij} + (\rho_{ij})^2 = 1$ [16]. By using this procedure on both eq. 2.16 and eq. 2.20, two equations describing the E field on both sides of an interface is obtained:

$$E'_{ri} = \left(\frac{\rho_{ij}}{\tau_{ij}}\right) E_{lj} + \left(\frac{1}{\tau ij}\right) E_{rj} \tag{2.22}$$

$$E'_{li} = \left(\frac{1}{\tau_{ij}}\right) E_{lj} + \left(\frac{\rho_{ij}}{\tau ij}\right) E_{rj} \tag{2.23}$$

This could also be arranged in a matrix fashion:

$$\begin{pmatrix} E'_{li} \\ E'_{ri} \end{pmatrix} = \frac{1}{\tau_{ij}} \begin{pmatrix} 1 & \rho_{ij} \\ \rho_{ij} & 1 \end{pmatrix} \begin{pmatrix} E_{lj} \\ E_{rj} \end{pmatrix} \tag{2.24}$$

or

$$\mathbf{E}_i' = \mathbf{H}_{ij}\mathbf{E}_j \tag{2.25}$$

where $\mathbf{H}_{ij}$ is the matrix describing the fields transition over the interface between medium i and j, and given by:

$$\mathbf{H}_{ij} = \frac{1}{\tau_{ij}} \begin{pmatrix} 1 & \rho_{ij} \\ \rho_{ij} & 1 \end{pmatrix} \tag{2.26}$$

A similar procedure (not shown here) can be utilised to obtain a matrix for the transition through the medium j using a phase factor $e^{-\beta_j}$, resulting in a propagation matrix $\mathbf{L}_j$:

$$\mathbf{L}_j = \begin{pmatrix} e^{-\beta_j} & 0 \\ 0 & e^{-\beta_j} \end{pmatrix} \tag{2.27}$$

where β_j is given as

$$\beta_j = \frac{2\pi}{\lambda} n_j d_j cos(\theta_j) \tag{2.28}$$

By combining the $\mathbf{H}$ and $\mathbf{L}$ matrices of several layers, a total matrix for a full stack of layers is obtained.

$$\mathbf{H}_{12}\mathbf{L}_2\mathbf{H}_{23}\mathbf{L}_3...\mathbf{L}_{N-1}\mathbf{H}_{N-1,N} = \mathbf{S}_{1N} = \begin{pmatrix} S_{11} & S_{12} \\ S_{21} & S_{22} \end{pmatrix} \tag{2.29}$$

The reflectance from the stack is then given by:

$$R = \left| \frac{S_{12}}{S_{22}} \right|^2 \tag{2.30}$$

This reflectance is what is measured in an SPR experiment, and from the derivation it is clear that it is dependent on which materials the stack is composed of, the thickness of the materials, as well as the angle of illumination. By plotting the reflectance as a function of angle for the set of parameters presented in table 2.1, the SPR profile in fig. 2.4 is obtained.

Material	n	d
Glass	1.77	-
Chromium	1.77	1E-9
Gold	0.17-4.93i	40E-9
Mercapto acid	1.493	2E-9
Buffer	1.33156	-

Table 2.1:

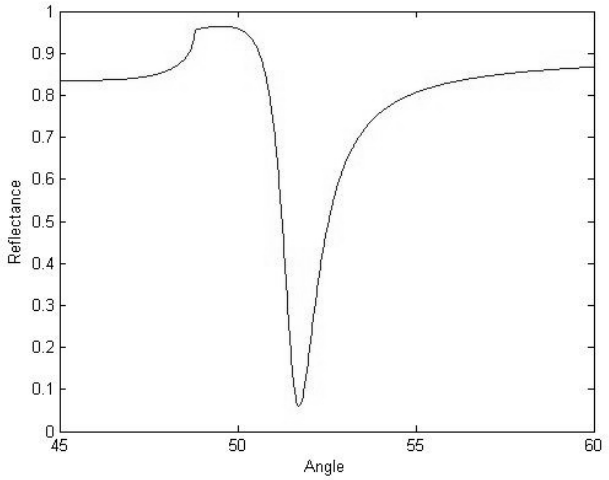

Figure 2.4: A theoretical SPR profile based on a matrix method for multiple-beam interference in multiple layers. The figure is produced by the Matlab code in sec. 2.4.

2.4 Matlab code

A Matlab code was produced to utilise the matrix method for multiple-beam interference, and this method is presented on the following pages.

```
close all
clear all

lambda_0=780E-9;
n_glass=1.77;
n_Cr=1.77;
n_Au=0.17-4.93i;      %Stenberg et al. 1991
n_Ma=1.493;           %målt ved 589nm @ 20 C
n_buffer=1.33156;     %HEPES buffer

d_Cr=1E-9;
d_Au=40E-9;
d_Ma=2E-9;

theta_start=45;       %Degree
theta_slut=60;        %Degree
thetasteps=1000;

n1=n_glass;
n2=n_Cr;
n3=n_Au;
n4=n_Ma;
n5=n_buffer;

eps1=n1^2;
eps2=n2^2;
eps3=n3^2;
eps4=n4^2;
eps5=n5^2;

k=2*pi/lambda_0;      %wave number

theta_start=theta_start/360*2*pi;
```

```
theta_slut=theta_slut/360*2*pi;
deltatheta=(theta_slut-theta_start)/(thetasteps-1);

for t=1:1:thetasteps
theta=theta_start+deltatheta*(t-1);

kx=k*n_glass*sin(theta);

kz1=sqrt(-(kx^2)+k^2*eps1);
if imag(kz1)>0,
    kz1=-kz1;
end
kz2=sqrt(-(kx^2)+k^2*eps2);
if imag(kz2)>0,
    kz2=-kz2;
end
kz3=sqrt(-(kx^2)+k^2*eps3);
if imag(kz3)>0,
    kz3=-kz3;
end
kz4=sqrt(-(kx^2)+k^2*eps4);
if imag(kz4)>0,
    kz4=-kz4;
end
kz5=sqrt(-(kx^2)+k^2*eps5);
if imag(kz5)>0,
    kz5=-kz5;
end

beta_Cr=kz2*d_Cr;   %2*pi/lambda_0*(n_Cr*d_Cr*cos(theta));
beta_Au=kz3*d_Au;  %2*pi/lambda_0*(n_Au*d_Au*cos(theta));
beta_Ma=kz4*d_Ma;  %2*pi/lambda_0*(n_Ma*d_Ma*cos(theta));

L_Cr=zeros(2);
L_Cr(1,1)=exp(-1i*beta_Cr);
L_Cr(2,2)=exp(1i*beta_Cr);

L_Au=zeros(2);
L_Au(1,1)=exp(-1i*beta_Au);
L_Au(2,2)=exp(1i*beta_Au);

L_Ma=zeros(2);
L_Ma(1,1)=exp(-1i*beta_Ma);
L_Ma(2,2)=exp(1i*beta_Ma);


b1=(n1/n2)^2*(kz2/kz1);
b2=(n2/n3)^2*(kz3/kz2);
b3=(n3/n4)^2*(kz4/kz3);
b4=(n4/n5)^2*(kz5/kz4);

rho_glass_Cr=(1-b1)/(1+b1);
rho_Cr_Au=(1-b2)/(1+b2);
rho_Au_Ma=(1-b3)/(1+b3);
rho_Ma_buffer=(1-b4)/(1+b4);

tau_glass_Cr=(2*(n1/n2))/(1+b1);
tau_Cr_Au=(2*(n2/n3))/(1+b2);
tau_Au_Ma=(2*(n3/n4))/(1+b3);
tau_Ma_buffer=(2*(n4/n5))/(1+b4);

H_glass_Cr=ones(2)/tau_glass_Cr;
```

```
H_glass_Cr(1,2)=rho_glass_Cr/tau_glass_Cr;   %rho is reflection coefficients
H_glass_Cr(2,1)=rho_glass_Cr/tau_glass_Cr;   %rho is reflection coefficients

H_Cr_Au=ones(2)/tau_Cr_Au;
H_Cr_Au(1,2)=rho_Cr_Au/tau_Cr_Au;          %rho is reflection coefficients
H_Cr_Au(2,1)=rho_Cr_Au/tau_Cr_Au;          %rho is reflection coefficients

H_Au_Ma=ones(2)/tau_Au_Ma;
H_Au_Ma(1,2)=rho_Au_Ma/tau_Au_Ma;          %rho is reflection coefficients
H_Au_Ma(2,1)=rho_Au_Ma/tau_Au_Ma;          %rho is reflection coefficients

H_Ma_buffer=ones(2)/tau_Ma_buffer;
H_Ma_buffer(1,2)=rho_Ma_buffer/tau_Ma_buffer;        %rho is reflection coefficients
H_Ma_buffer(2,1)=rho_Ma_buffer/tau_Ma_buffer;        %rho is reflection coefficients

S_glass_buffer=H_glass_Cr*L_Cr*H_Cr_Au*L_Au*H_Au_Ma*L_Ma*H_Ma_buffer;

R_list(1,t)=(abs(S_glass_buffer(1,2)/S_glass_buffer(2,2)))^2;
vinkel(t)=theta/(2*pi)*360;
end

figure;
plot(vinkel,R_list)
```

This is a sample of the most condensed form of the code, and several different variations have been produced. Two of these can be seen in appendix B. From these programs it can be deduced, that a change of 0.01 in the refractive index corresponds to having coated the chip with 33 nm. of a organic layer. From a calibration of the SPR set-up performed by Kasper Risgaard Jensen (data not shown) a change of 0.01 in the refractive index corresponds to a shift in the signal of 25.4 pixels, thus a change of one pixel indicates that a organic layer of 1.2 nm. have been added.

2.5 Considerations for chip design

SPR surfaces have some general considerations to take into account. The gold layer on the chip should be between 30 and 60 nm. [17, 18], and a 1 nm. chromium layer should be applied between the glass and the gold, to facilitate adhesion of the gold [18]. According to the simulations performed in this work, the optimal gold thickness should be between 40 and 50 nm. as seen in fig. 2.5. Based on experiences the gold thickness is set to 40 nm. for the sensor used in this project.

To immobilise the sensor molecules on the surface a linker is needed. A well tested method is to utilise a mercapto acid monolayer and link this to the bio molecule with a 1-ethyl-3-(3-dimethylaminopropyl)carbodiimide / N-Hydroxysuccinimide (abbreviated EDC/NHS) activation to link the mercapto acid to the antibody [19, 1]. In this Work 16-Mercaptohexadecanoic acid is utilised as a linker, and antibodies specific to cTnI (anti cTnI) was supplied by Radiometer Medical ApS. to be utilised as sensor molecule.

An alternative surface is acquired from Xantec bioanalytics GmbH. This surface is coated with a carboxymethysdextran hydrogel with a thickness of approximately 500 nm. This gel is also compatible with the EDC/NHS activation for antibody binding. The gel structure of the surface should provide for

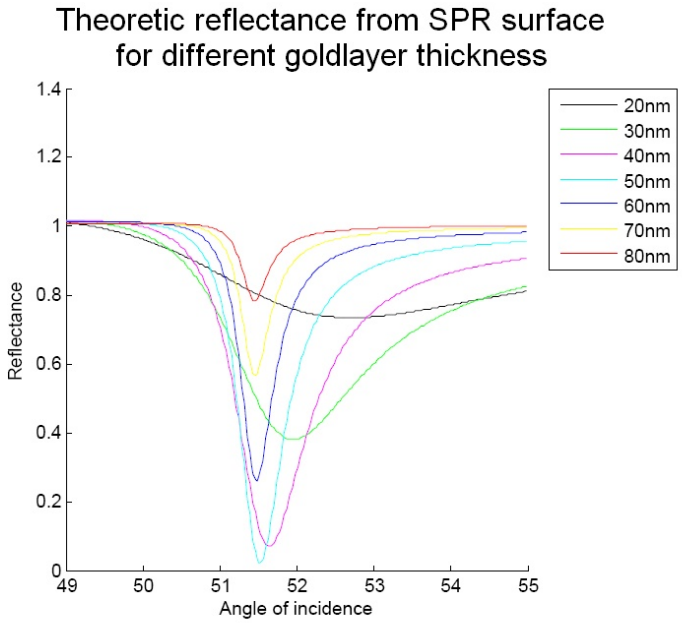

Figure 2.5: Theoretical reflection profile from an SPR surface based on the multiple beam interference method 2.3. as a deep and narrow dip is the optimal condition, it is seen than the optimal gold layer thickness is between 40 and 50 nm.

a larger number of antibodies immobilised on the surface, and thus potential for a stronger SPR signal.

Materials and Methods 3

3.1 SPR chip production

500 μm thick Borofloat glass wafers, double side polished, 60/40 scratch/dig, attained from University Wafers Ltd. was rinsed with acetone (two minutes sonification) and fumic nitric acid (two minutes sonification), washed with H_2O, and dried with N_2. The wafer was then exposed to one minute of oxygen plasma, and subsequently rinsed with acetone and 2-propanol and dried with N_2 before being mounted in the sputter.

A scientific vacuum system 2400 sputter was utilized to deposit 1 nm. Cr (7 sec. @ 400 W) and 40 nm. Au (87 sec. @ 100 W) at a pressure of 0.05 $mbar$. Trials on 1·1 cm silicon wafers were performed to determine the time needed for chromium deposition, where chromium thickness were determined by ellipsometry (multiple angle (60-70-80°))with a range of 320-820 nm. Based on these trials, the sputtering time for chromium was set to 7 sec. A sputtering time of six sec. is not enough to open the shutter, but as soon the shutter is open, the sputtering rate is 1.15 $nm\ s^{-1}$ as seen on fig. 3.1.

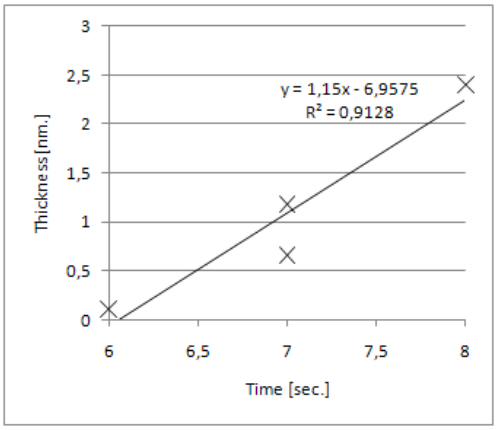

Figure 3.1: Chromium thickness as a function of sputtering time with a linear tendency line. The equation shows that the sputtering rate after shutter opening is approximately 1.1 $nm\ s^{-1}$.

The wafer is removed from the sputtering chamber, and the gold surface is spin coated with a thin layer of photo resist, to protect the surface. A Disco Automatic Dicing saw 321 is utilised to cut the wafer into $1.1cm \cdot 1.1cm$ SPR chips. Subsequently the resist is removed, and the chips is rinsed with acetone and 2-propanol, and dried with n_2

3.2 Antibody immobilisation

In order to create the sensor surface with immobilized antibodies, the chip is first exposed to 15 minutes of UV light, and subsequently submerged in 99,9% ethanol for 15 minutes. After being blowdried with N_2 gas, the chip is mounted in the SPR setup.

The flow rate is set to 20 $\mu l/min.$ and the buffer syringe is loaded with $5mM\ NaOAc\ pH$ 5.0. The buffer is left running for 10 minutes, and a 5

minutes injection of $2M\ NaCl/$ 10 $mM\ NaOH\ pH$ 9.3, hereafter abbrivated $NaCl/NaOH$, followed by 80 minutes buffer injection for sensor equilibration. A 5 minutes injection of a 0.1 % Tween 20 is injected to rince the surface, followed by two 5 minutes injections of Milli Q H_2O. Between each of these injections are an 11 minutes buffer flow, and after the second Milli Q H_2O injection, the buffer is left running for 4 minutes.

To facilitate the antibody binding, a mono layer of 16-Mercaptohexadecanoic acid is formed on the surface by injecting 1 ml of a 25 mM solution, and changing the flow rate to 5 $\mu l/min$. After 2.5 hour, the flow rate is adjusted back to 20 $\mu l/min$. and a series of 5 minutes rinsing injections are performed with 4 minutes of buffer in between. The order of rinsing injections is first a $EtOH$ injection followed by a $NaCl/NaOH$ injection, two more injections of $EtOH$, and lastly an injection of $NaCl/NaOH$. To activate the 16-Mercaptohexadecanoic acid a 8 min. injection of 0.5 M EDC / 0.5 M NHS solution in a 0.5 M MES buffer (EDC/NHS) is performed. Immediately after the flow is stopped, and a 5 mM acetic acid solution is injected for 2 min. and the flow is stopped again to rewire the flow around the secondary flow chamber. The antibody (anti cTnI) solution (25 $\mu g/ml$) is injected for 30 min. followed by 5 min. buffer. After stopping the flow and rewiring, a 20 min. injection of Milli Q H_2O is performed, and finally a 15 min. injection of a 1 M ethanol amine pH 8.8 is performed to block residual 16-Mercaptohexadecanoic acid.

For employing the sensor, the buffer is changed to a 10 mM HEPES, 150 $mM\ NaCL$ 3.4 mM EDTA, 0.05 % Tween 20 pH 7.4 (abbrivated HEPES), and one 6 min. injection of $NaCl/NaOH$ and 5 5 min. injections of $NaOAc$ is applied to rince and equilibrate the system. A protocol for the preparation and immobilisation can be seen en appendix A

The chips bought from Xantec is prepared with a low weight dextran layer with a thickness of aproximately 500 nm, and ready to be EDC/NHS activated. The chip is mounted in the SPR setup, and the same procedure described above from the EDC/NHS activation, and subsequent antibody immobilisation is utilised.

3.3 Antigen binding

To measure the antigen binding, the system is first equilibrated with HEPES buffer for approximately one hour, or until the signal is steady. Each sample injection takes 10 minutes, and an injection for 5 minutes of 20 mM phosphoric acid pH 2.5 is utilised to reset the sensor (unbind the antigen). Between injections a 6 minutes delay is necessary to allow the signal to return to normal, and rinse the injection loop.

The cTnI is supplied from Radiometer Medical aps in a 30 ng/ml solution in BSA, and samples are prepared in the following concentrations: 10 ng/ml; $8ng/ml$; $6ng/ml$; $4ng/ml$; $2ng/ml$; $1ng/ml$; $0.5ng/ml$;

For the measurements with the xantec surface, a sample with a concentration of 0.1 ng/ml s also prepared. All samples are prepared in 3 copies, and data from each series is collected in the same datafile, and the samples are injected in a random order. In each series two or three 'blank' reference injections of buffer without cTnI are performed during the series.

For the measurements on the mercapto acid chip, cTnI is diluted in HEPES

buffer, and for the measurements on the xantec chip, the cTnI is first diluted in HEPES, and after these measurements, a new set of samples is prepared, where cTnI is diluted in BSA.

Results 4

4.1 Antibody immobilisation

From section 2.4 we have that a change of one pixel indicates a change of 1.2 nm. For the chip with 16-mercaptohexadecanoic acid coating, the baseline before the injection of 16-mercaptohexadecanoic acid had a value of 252.50. After formation of the monolayer, and rinsing with ethanol, the baseline is at 256.77 pixels. The shift changed 4,27 pixels translating into formation of an organic layer with a thickness of 5.12 nm. This seems unlikely, but may just be a result of a small uncertainty in the value of the refractive index used in the theoretical model. After the immobilisation of anti cTnI the shift changed 5.39 pixels, indicating a organic layer of additionally 6.47 nm.

For the xantec chip, the change from before and after the immobilisation of anti cTnI was 6.25 pixels or a 7.5 nm thick layer.

4.2 Antigen binding

The raw data from the SPR setup is first loaded into SPRV4's Post processing program, and the data from the injections are manually extracted from both data channels. The data is then exported to Scrupper2 from BioLogic Software, where the data is zeroed, aligned and the reference signal is subtracted. The reference injections are also identified, and subtracted from the signal, and the response as a function of antigen concentration is found.

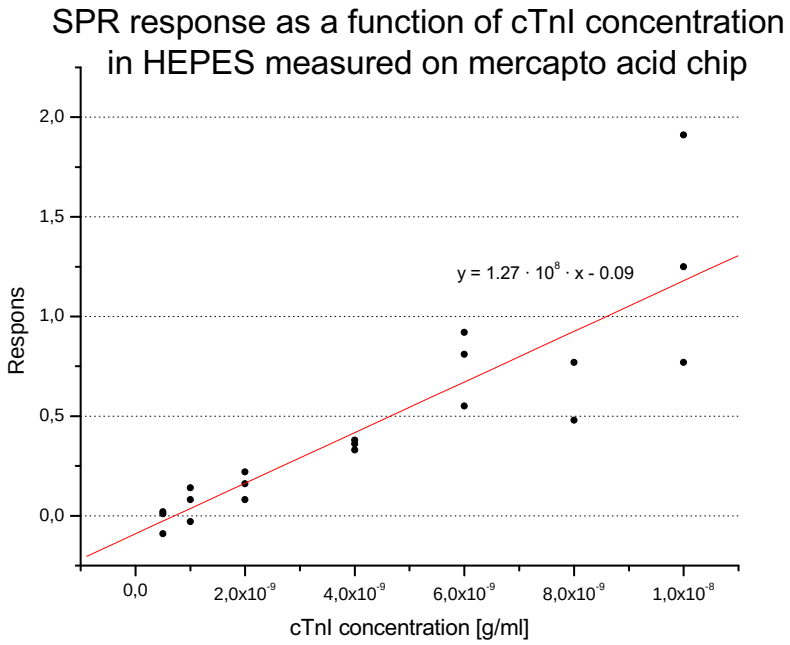

Figure 4.1: SPR respons as a function of cTnI concentration. These measurements was performed with a mercaptohehadecanoicacid sensor surface. cTnI is diluted in HEPES buffer.

Figure 4.1 shows a linear tendency between cTnI concentration and SPR response from the mercapto acid chip. However there seems to be a heteroscedasticity tendency, as the datapoints distance from the tendency line increase at higher concentrations. Also the sensors response at concentrations lower than 2 ng/ml may not be valid as negative signals are observed.

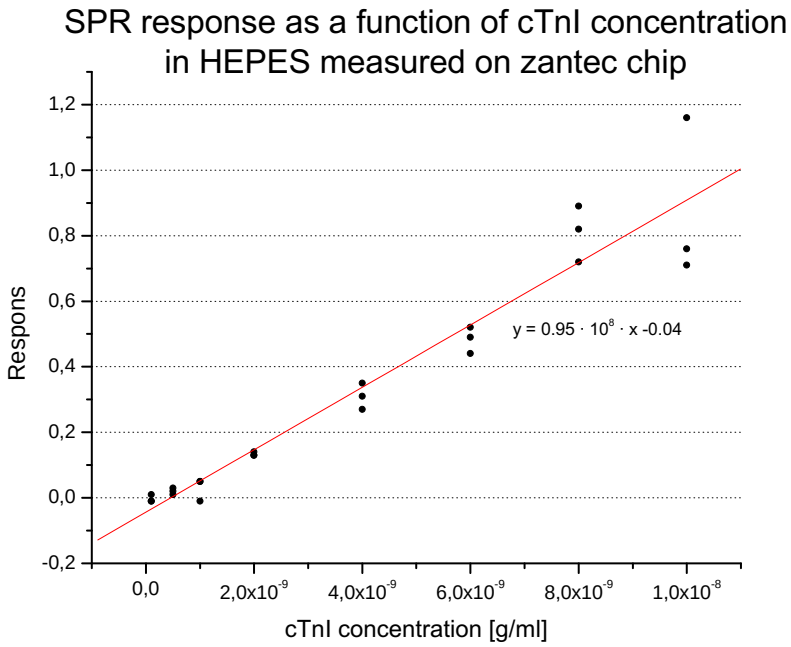

Figure 4.2: SPR respons as a function of cTnI concentration. These measurements was performed with a SPR Sensorchip CMD500l sensor surface from Xantec bioanalytics. cTnI is diluted in HEPES buffer.

The xantec chip shows a more consistent signal between series, as the datapoints are closer together, and closer to the tendency line, as seen in figure 4.2. The data points for 10 ng/ml are diverting trom the general tendency, as two of them are significantly lower than the tendency would suggest. If the two lower datapoints at 10 ng/ml disregarded as invalid, the tendency seems more exponential than linear. However the data from six to ten ng/ml seems linear, and if a tendency line is extrapolated, it intersects the zero response line at approximately 3 ng/ml, which according to Eggins [2], would be the lower limit of detection.

Figure 4.3 shows unlike the previous two experiments no clear tendency, and a large spread in signal strength. This indicates that the sensor is unable to measure the concentration of cTnI properly.

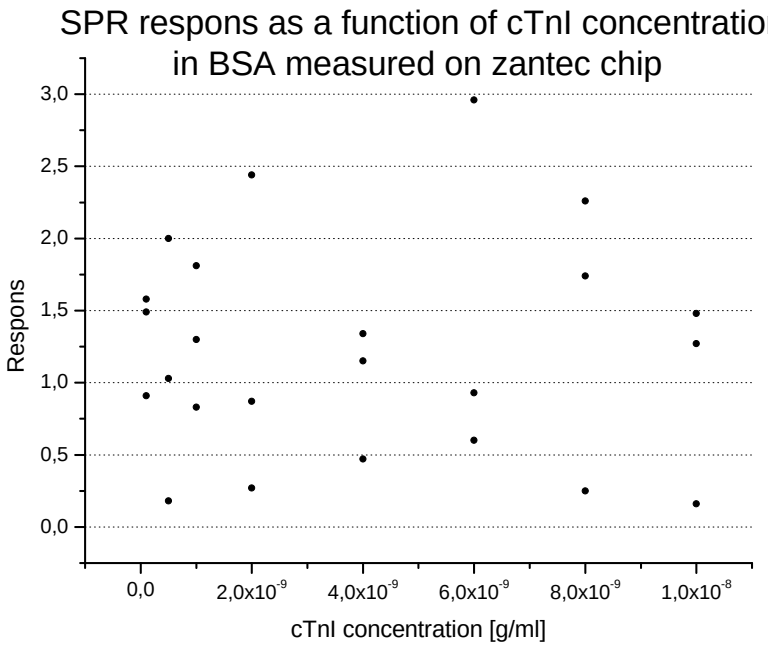

Figure 4.3: SPR respons as a function of cTnI concentration. These measurements was performed with a SPR Sensorchip CMD500l sensor surface from Xantec bioanalytics. cTnI is diluted in BSA.

Discussion 5

The mercapto acid chip shows some clear tendencies in the correlation between cTnI concentration and SPR response. However the heteroscedasticity indicates that the accuracy and reproducibility of the sensor may not be optimal. From the data obtained in this project, a lower limit of detection could not be determined. From the immobilisation procedure the changes in the resonance shift is utilised in unison with the matlab model to give an estimation of the amount of both mercapto acid and antigen bound. The models prediction of the thickness of the mercapto acid layer to be 5.12 nm thick is most likely inaccurate, as 16-Mercaptohexadecanoic acid is a 18 atoms long molecule. In the analysis of the thickness of the layer of anti cTnI immobilised, the estimation of 6.47 nm corresponds roughly with the 7.5 nm. estimated as the size of an antibody as described in section 2.1.

The Xantec SPR surface provides a carboxymethyldextran hydrogel for immobilising antibodies and the dextran matrix should provide for a more efficient immobilisation. According to the matlab model a layer of 7.5 nm antibody was immobilised, this does corresponds well with the thickness of an antibody, but as the hydrogel is 500 nm. thick, a signifficantly higher value was expected. The model was however not designed to simulate changes in a layer, and 500 nm. is roughly the extend of the evanescent EM field utilised in the sensor. Thus the measurerment of 7.5 nm may not be accurate. A point to notice is that the data indicates that more antibodies have been immobilised on the Xantec chip than on the mercapto chip.

The measurements performed with the xantec chip are somewhat divided. The data from the cTnI diluted in HEPES shows a clear tendency, and a lower limit of detection of 3 ng/ml is determined. The sensor shows a good reproducibility between the three series, and the heteroscedasticity observed with the mercapto chip is not observed.

When the measurements is repeated with cTnI diluted in BSA, the picture is however changed completely. There is no tendency at all, and almost no consistency between measurements. The large spread in responses could be caused by a saturation of the sensor with unspecific bound proteins from the BSA, that is adsorbed into the dextran gel regardless of them being bound to the antibody or not. Why this did not happen when cTnI was diluted in HEPES could be explained by pH values. When HEPES was utilised as dilution, the buffer properties would stabilise the pH, but the pH is not checked when diluting in BSA.

Conclusion and further perspectives

6

In this project a SPR immuno assay biosensor for detection of cTnI sample was created. Two different surfaces was obtained and tested, one utilising 16-mercaptohexadecanoic acid for immobilisation of anti cTnI, and one utilising a carboxymethyldextran hydrogel for immobilisation. For the purpose of evaluating the amount of antibody immobilised, a matrix model for multiple layer interference is utilised to create a matlab code for modelling the signal from a SPR surface.

It was found that both sensors was able to detect cTnI diluted in HEPES buffer, however the hydrogel coated surface provided the best results with better reproducibility. When the cTnI was diluted in BSA, the results was however rather discouraging as no clear tendency was observable. The reason for this may be a change in pH value from the HEPES buffer to the BSA, thus changing the charges of the molecules on the solution, and allowing random proteins to bind unspecific to the surface and saturating the sensor.

For further experiments in this area it could be interesting to test if a change in pH value could improve the sensors performance, or test if a different hydrogel could avoide unspecific binding of proteins.

Another interesting method was reproted by Liu *et al.* [17] where a gold nanoparticle is integrated into the linker to significantly increase the sensitivity of the sensor.

Protcol for SPR chip Preparation

A

Protocol for SPR chip preparation

Flowrate: 20 $\mu l/min$

Buffer: NaOAc 5 mM pH 5.0

	10 min	Buffer
	5 min	NaCl/NaOH
	80 min	Buffer
	5 min	0.1% Tween 20
	5 min	Buffer
	5 min	H_2O
	11 min	Buffer
	5 min	H_2O
	4 min	Buffer
		Flow rate: 5 $\mu l/min$
	2.5 hour	1 ml. 25 mM solution 16-Mercapto hexadecanoic acid (time is minimum)
		Flow rate: 20 $\mu l/min$
	4 min	Buffer
	5 min	EtOH
	4 min	Buffer
	5 min	NaCl/NaOH
	4 min	Buffer
	5 min	EtOH
	4 min	Buffer
	5 min	EtOH
	4 min	Buffer
	5 min	NaCl/NaOH
		Buffer
	8 min	EDC/NHS
		Stop flow
	2 min	Acetic acid
		Stop Flow – Rewire
	30 min	Antibody solution 25 $\mu g/ml$
	5 min	Buffer
		Stop Flow – Rewire
	10 min	Milli Q
	4 min	Buffer
	10 min	Milli Q
	4 min	Buffer
	15 min	1 M ethanol Amine pH 8.8
		Stop Flow Change buffer to HEPES Start Flow
	20 min	Buffer
	6 min	Coupling buffer
	30 min	Buffer

Matlab programs B

two of the programs utilised during this project.

B.0.1 Profile as function of gold layer thickness

This program was utilised for creating figure 2.5.

```
function SPR_matrix_profile_comparison_v2
close all
clear all

%variables
n_Ma=1.493;       %målt ved 589nm @ 20 C
n_buffer=1.33156; %HEPES buffer

d_Ma=1E-9;

%vinkel ting
theta_start=49.01;       %GRADER!!
theta_slut=54.99;        %GRADER!!
thetasteps=250;

theta_start=theta_start/360*2*pi;
theta_slut=theta_slut/360*2*pi;
deltatheta=(theta_slut-theta_start)/(thetasteps-1);


for t=1:1:thetasteps;
    theta=theta_start+deltatheta*(t-1);
    vinkel(t)=theta/(2*pi)*360;
end

figure(1);
hold on
for l=2:8
d_Au=l*10E-9
[R_list]=spr_calc(n_Ma,n_buffer,d_Ma,d_Au,vinkel,theta_start,theta_slut,deltatheta,thetas
% [y_data]=data_import(vinkel);


if l==2
plot(vinkel,R_list,'k')
end
if l==3
plot(vinkel,R_list,'g')
end
if l==4
plot(vinkel,R_list,'m')
end
if l==5
plot(vinkel,R_list,'c')
end
if l==6
plot(vinkel,R_list,'b')
end
if l==7
plot(vinkel,R_list,'y')
end
```

```
if l==8
plot(vinkel,R_list,'r')
end



end

%axis([theta_start*180/pi theta_slut*180/pi+1e-3 0 1])
legend('20nm','30nm','40nm','50nm','60nm','70nm','80nm','Location','NorthEastOutside')
%legend('n_3=1.3300','n_3=1.3340','n_3=1.3380','n_3=1.3420','n_3=1.3460','n_3=1.3500','L
xlabel('Angle of incidence')
ylabel('Reflectance')

load SPR_data.txt;
[sx,sy]=size(SPR_data);

for i=1:250
    y_data(i)=SPR_data(i+150,2)/7E4;
    %x_data(i)=i;
end


% options = fitoptions('NonlinearLeastSquares',method);
%
%
% [fresult,gof,fout]=fit(vinkel,y_data,spr_calc,options);

%figure(1);
%hold on
%plot(vinkel,R_list)

%hold on;
%figure(1);
%plot(vinkel,R_list)

%figure(2);
%plot(vinkel,y_data);

%figure(2);
%plot(vinkel,R_list-y_data);



end



function [R_list] = spr_calc(n_Ma,n_buffer,d_Ma,d_Au,vinkel,theta_start,theta_slut,deltat

lambda_0=780E-9;
n_glass=1.77;
n_Cr=3.11982+3.44408i; % http://refractiveindex.info/?group=METALS&material=Chromium d. 1

n_Au=0.17-4.93i;   %Stenberg et al. 1991

n_Ma=n_Ma;
n_buffer=n_buffer;


d_Cr=1E-9;
d_Au=d_Au;
```

```
d_Ma=d_Ma;


% theta_start=51;          %GRADER!!
% theta_slut=55;          %GRADER!!
% thetasteps=250;

n1=n_glass;
n2=n_Cr;
n3=n_Au;
n4=n_Ma;
n5=n_buffer;


eps1=n1^2;
eps2=n2^2;
eps3=n3^2;
eps4=n4^2;
eps5=n5^2;


k=2*pi/lambda_0;


% theta_start=theta_start/360*2*pi;
% theta_slut=theta_slut/360*2*pi;
% deltatheta=(theta_slut-theta_start)/(thetasteps-1);



for t=1:1:thetasteps
theta=theta_start+deltatheta*(t-1);


kx=k*n_glass*sin(theta);

kz1=sqrt(-(kx^2)+k^2*eps1);
if imag(kz1)>0,
    kz1=-kz1;
end
kz2=sqrt(-(kx^2)+k^2*eps2);
if imag(kz2)>0,
    kz2=-kz2;
end
kz3=sqrt(-(kx^2)+k^2*eps3);
if imag(kz3)>0,
    kz3=-kz3;
end
kz4=sqrt(-(kx^2)+k^2*eps4);
if imag(kz4)>0,
    kz4=-kz4;
end
kz5=sqrt(-(kx^2)+k^2*eps5);
if imag(kz5)>0,
    kz5=-kz5;
end


beta_Cr=kz2*d_Cr;   %2*pi/lambda_0*(n_Cr*d_Cr*cos(theta));
beta_Au=kz3*d_Au;  %2*pi/lambda_0*(n_Au*d_Au*cos(theta));
beta_Ma=kz4*d_Ma;  %2*pi/lambda_0*(n_Ma*d_Ma*cos(theta));
```

```
L_Cr=zeros(2);
L_Cr(1,1)=exp(-1i*beta_Cr);
L_Cr(2,2)=exp(1i*beta_Cr);

L_Au=zeros(2);
L_Au(1,1)=exp(-1i*beta_Au);
L_Au(2,2)=exp(1i*beta_Au);

L_Ma=zeros(2);
L_Ma(1,1)=exp(-1i*beta_Ma);
L_Ma(2,2)=exp(1i*beta_Ma);


b1=(n1/n2)^2*(kz2/kz1);
b2=(n2/n3)^2*(kz3/kz2);
b3=(n3/n4)^2*(kz4/kz3);
b4=(n4/n5)^2*(kz5/kz4);


rho_glass_Cr=(1-b1)/(1+b1);
rho_Cr_Au=(1-b2)/(1+b2);
rho_Au_Ma=(1-b3)/(1+b3);
rho_Ma_buffer=(1-b4)/(1+b4);

tau_glass_Cr=(2*(n1/n2))/(1+b1);
tau_Cr_Au=(2*(n2/n3))/(1+b2);
tau_Au_Ma=(2*(n3/n4))/(1+b3);
tau_Ma_buffer=(2*(n4/n5))/(1+b4);


H_glass_Cr=ones(2)/tau_glass_Cr;
H_glass_Cr(1,2)=rho_glass_Cr/tau_glass_Cr;   %rho is reflection coefficients
H_glass_Cr(2,1)=rho_glass_Cr/tau_glass_Cr;   %rho is reflection coefficients

H_Cr_Au=ones(2)/tau_Cr_Au;
H_Cr_Au(1,2)=rho_Cr_Au/tau_Cr_Au;          %rho is reflection coefficients
H_Cr_Au(2,1)=rho_Cr_Au/tau_Cr_Au;          %rho is reflection coefficients

H_Au_Ma=ones(2)/tau_Au_Ma;
H_Au_Ma(1,2)=rho_Au_Ma/tau_Au_Ma;          %rho is reflection coefficients
H_Au_Ma(2,1)=rho_Au_Ma/tau_Au_Ma;          %rho is reflection coefficients

H_Ma_buffer=ones(2)/tau_Ma_buffer;
H_Ma_buffer(1,2)=rho_Ma_buffer/tau_Ma_buffer;       %rho is reflection coefficients
H_Ma_buffer(2,1)=rho_Ma_buffer/tau_Ma_buffer;       %rho is reflection coefficients



S_glass_buffer=H_glass_Cr*L_Cr*H_Cr_Au*L_Au*H_Au_Ma*L_Ma*H_Ma_buffer;



R_list(1,t)=(abs(S_glass_buffer(1,2)/S_glass_buffer(2,2)))^2;

% vinkel(t)=theta/(2*pi)*360;


end

% figure(1);
% hold on
% plot(vinkel,R_list)
```

```
% [sy, sx]=size(R_list);
%
% for i=1:(sx-5)
%     theta=theta_start+deltatheta*(i-1);
%     diff_R_list(i)=(-R_list(i)+R_list(i+5))/(5);
%     diff_vinkel(i)=theta/(2*pi)*360;
% end
%
% for i=1:(sx-6)
%     theta=theta_start+deltatheta*(i-1);
%     if sign(diff_R_list(i))==sign(diff_R_list(i+1))
%         signchange(i)=0;
%     else
%         sign_note=theta/(2*pi)*360
%     end
% end
%
% figure(2)
% plot(diff_vinkel, diff_R_list)


end



function [y_data] = data_import(vinkel)

load SPR_data.txt;
[sx, sy]=size(SPR_data);

for i=1:250
    y_data(i)=SPR_data(i+150,2)/7E4;
    %x_data(i)=i;
end

x_data=vinkel;
% hold on;
%
% figure(2);
% plot(x_data, y_data)

end
```

B.0.2 Profile, and the differentiated function

This program was utilised to calculate the correlation between the thickness of the gold layer, and the resonance angle.

```
function SPR_matrix_profile_derivative
close all
clear all


spr_calc;
%data_import;

%hold on;
%figure(1);
%plot(vinkel,R_list)

%figure(2);
%plot(x_data,y_data);

end


function spr_calc

lambda_0=780E-9;
n_glass=1.77;
n_Cr=1.77;

n_Au=0.17-4.93i;    %Stenberg et al. 1991

n_Ma=1.493;         %målt ved 589nm @ 20 C
n_buffer=1.33156; %HEPES buffer



d_Cr=1E-9;
d_Au=40E-9;
d_Ma=10E-9;



theta_start=45;         %GRADER!!
theta_slut=60;          %GRADER!!
thetasteps=768;

n1=n_glass;
n2=n_Cr;
n3=n_Au;
n4=n_Ma;
n5=n_buffer;


eps1=n1^2;
eps2=n2^2;
eps3=n3^2;
eps4=n4^2;
eps5=n5^2;


k=2*pi/lambda_0;
```

```
theta_start=theta_start/360*2*pi;
theta_slut=theta_slut/360*2*pi;
deltatheta=(theta_slut-theta_start)/(thetasteps-1);



for t=1:1:thetasteps
theta=theta_start+deltatheta*(t-1);


kx=k*n_glass*sin(theta);

kz1=sqrt(-(kx^2)+k^2*eps1);
if imag(kz1)>0,
    kz1=-kz1;
end
kz2=sqrt(-(kx^2)+k^2*eps2);
if imag(kz2)>0,
    kz2=-kz2;
end
kz3=sqrt(-(kx^2)+k^2*eps3);
if imag(kz3)>0,
    kz3=-kz3;
end
kz4=sqrt(-(kx^2)+k^2*eps4);
if imag(kz4)>0,
    kz4=-kz4;
end
kz5=sqrt(-(kx^2)+k^2*eps5);
if imag(kz5)>0,
    kz5=-kz5;
end


beta_Cr=kz2*d_Cr;   %2*pi/lambda_0*(n_Cr*d_Cr*cos(theta));
beta_Au=kz3*d_Au;  %2*pi/lambda_0*(n_Au*d_Au*cos(theta));
beta_Ma=kz4*d_Ma;  %2*pi/lambda_0*(n_Ma*d_Ma*cos(theta));

L_Cr=zeros(2);
L_Cr(1,1)=exp(-1i*beta_Cr);
L_Cr(2,2)=exp(1i*beta_Cr);

L_Au=zeros(2);
L_Au(1,1)=exp(-1i*beta_Au);
L_Au(2,2)=exp(1i*beta_Au);

L_Ma=zeros(2);
L_Ma(1,1)=exp(-1i*beta_Ma);
L_Ma(2,2)=exp(1i*beta_Ma);


b1=(n1/n2)^2*(kz2/kz1);
b2=(n2/n3)^2*(kz3/kz2);
b3=(n3/n4)^2*(kz4/kz3);
b4=(n4/n5)^2*(kz5/kz4);


rho_glass_Cr=(1-b1)/(1+b1);
rho_Cr_Au=(1-b2)/(1+b2);
rho_Au_Ma=(1-b3)/(1+b3);
rho_Ma_buffer=(1-b4)/(1+b4);
```

```
tau_glass_Cr=(2*(n1/n2))/(1+b1);
tau_Cr_Au=(2*(n2/n3))/(1+b2);
tau_Au_Ma=(2*(n3/n4))/(1+b3);
tau_Ma_buffer=(2*(n4/n5))/(1+b4);


H_glass_Cr=ones(2)/tau_glass_Cr;
H_glass_Cr(1,2)=rho_glass_Cr/tau_glass_Cr;   %rho is reflection coefficients
H_glass_Cr(2,1)=rho_glass_Cr/tau_glass_Cr;   %rho is reflection coefficients

H_Cr_Au=ones(2)/tau_Cr_Au;
H_Cr_Au(1,2)=rho_Cr_Au/tau_Cr_Au;          %rho is reflection coefficients
H_Cr_Au(2,1)=rho_Cr_Au/tau_Cr_Au;          %rho is reflection coefficients

H_Au_Ma=ones(2)/tau_Au_Ma;
H_Au_Ma(1,2)=rho_Au_Ma/tau_Au_Ma;          %rho is reflection coefficients
H_Au_Ma(2,1)=rho_Au_Ma/tau_Au_Ma;          %rho is reflection coefficients

H_Ma_buffer=ones(2)/tau_Ma_buffer;
H_Ma_buffer(1,2)=rho_Ma_buffer/tau_Ma_buffer;       %rho is reflection coefficients
H_Ma_buffer(2,1)=rho_Ma_buffer/tau_Ma_buffer;       %rho is reflection coefficients



S_glass_buffer=H_glass_Cr*L_Cr*H_Cr_Au*L_Au*H_Au_Ma*L_Ma*H_Ma_buffer;



R_list(1,t)=(abs(S_glass_buffer(1,2)/S_glass_buffer(2,2)))^2;

vinkel(t)=theta/(2*pi)*360;


end

figure(1);
hold on
plot(vinkel,R_list)

[sy,sx]=size(R_list);

for i=1:(sx-5)
    theta=theta_start+deltatheta*(i-1);
    diff_R_list(i)=(-R_list(i)+R_list(i+5))/(5);
    diff_vinkel(i)=theta/(2*pi)*360;
end

for i=1:(sx-6)
    theta=theta_start+deltatheta*(i-1);
    if sign(diff_R_list(i))==sign(diff_R_list(i+1))
        signchange(i)=0;
    else
        sign_note=theta/(2*pi)*360
    end
end

figure(2)
plot(diff_vinkel,diff_R_list)


end
```

```
function data_import

load SPR_data.txt;
[sx,sy]=size(SPR_data);

for i=1:sx
    y_data(i)=SPR_data(i,2);
    x_data(i)=i;
end

figure(2);
plot(x_data,y_data)

end
```

Bibliography

[1] Jingyan Wei, Ying Mu, Daqian Song, Xuexun Fang, Xia Liu, Lisha Bu, Hanqi Zhang, Guizhen Zhang, Jiahua Ding, Weizhong Wang, Qinhan Jin, and Guimin Luo. A novel sandwich immunosensing method for measuring cardiac troponin i in sera. *Analytical Biochemistry*, 321:209–216, October 2007.

[2] Brian R. Eggins. *Chemical sensors and biosensors.* Wiley, 2002. ISBN: 978-0-471-89914-3.

[3] Jirí Homola. *Surface plasmon resonance based sensors.* Springer, 1nd edition, 2006. ISBN: 978-3-540-33918-2.

[4] Anna J. Tudos Richard B. M. Schasfoort. *Handbook of Surface Plasmon Resonance.* RSC Publishing, 1nd edition, 2008. ISBN: 978-0-85404-267-8.

[5] American Heart Association. *Heart Attack and Angina Statistics.* 1.8.20010. http://www.americanheart.org/presenter.jhtml?identifier=4591.

[6] Lauro Tatsuo Kubota Rosa Fireman Dutra. An spr immunosensor for human cardiac troponin t using specific binding avidin to biotin at carboxymethyldextran-modified godl chip. *Clinica Chimica*, 376:114–120, February 2007.

[7] Lubert Stryer Jeremy M. Berg, John L. Tymoczko. *Biochemistry.* W. H. Freeman and Company, 6th edition, 2007. ISBN: 0-7167-8724-5.

[8] Nenad Ban, Carlos Escobar, Robyn Carcia, Karl Hasel, John Day, and Aaron Greenwood. Crystal structure of an idiotype-anti-idiotype fab complex. *Proc. Natl. Acad. sci. USA*, 91:1604–1608, March 1994.

[9] JMichael J.E. Sternberg. *Protein structure prediction.* Oxford university press, 2002. ISBN: 0-19-963496-3.

[10] Peter S. Hansen. *Monoclonal antibody-based Surface Plasmon Resonance sensors for pathogen detection.* Biocentrum-DTU, 2007. ISBN: 87-91494-44-3.

[11] Shuming Nie, Yun Xing, Gloria J. Kim, and Jonathan W. Simons. Nanotechnology applications in cancer. *Annual Review of Biomedical Engineering*, 9(1):257–288, 2007.

[12] Karen R Steingart, Megan Henry, Suman Laal, Philip C Hopewell, Andrew Ramsay, Dick Menzies, Jane Cunningham, Karin Weldingh, and

Madhukar Pai. Commercial serological antibody detection tests for the diagnosis of pulmonary tuberculosis: A systematic review. *PLoS Med*, 4, 06 2007.

[13] Richard G. Smith, Natasha D'Souza, and Stephen Nicklin. A review of biosensors and biologically-inspired systems for explosives detection. *The Analyst*, 133(5):571–584.

[14] Paul J. Conroy, Stephen Hearty, Paul Leonard, and Richard J. O'Kennedy. Antibody production, design and use for biosensor-based applications. *Seminars in Cell & Developmental Biology*, 20(1):10–26, February 2009.

[15] Stephan A. Maier. *Plasmonics: Fundamentals and Applications*. Springer, 2007. ISBN: 0-388-33150-6.

[16] Thomas E. Furtak Miles V. Klein. *Optics*. Wiley, 2nd edition, 1986. ISBN: 0-471-87297-0.

[17] Daqian Song Qinglin Zhang Yuan Tian Xia Liu, Ying Sun and Hanqi Zhang. Enhanced optical immunosensor based on surface plasmon resonance for determination of transferrin. *Talanta*, 68:1026–1031, January 2006.

[18] Alastair W. Wark, Hye Jin Lee, and Robert M. Corn. Long-Range surface plasmon resonance imaging for bioaffinity sensors. *Analytical Chemistry*, 77(13):3904–3907, July 2005.

[19] Xia Liu, Jingyan Wei, Daqian Song, Ziwei Zhang, Hanqi Zhang, and Guimin Luo. Determination of affinities and antigenic epitopes of bovine cardiac troponin i (cTnI) with monoclonal antibodies by surface plasmon resonance biosensor. *Analytical Biochemistry*, 314(2):301–309, March 2003.